Evolution of phosphorus complexation and mineralogy during (hydro)thermal treatments of activated and anaerobically digested sludge: Insights from sequential extraction and P K-edge XANES

Rixiang Huang, Yuanzhi Tang[*]

School of Earth and Atmospheric Sciences, Georgia Institute of Technology, 311 Ferst Dr, Atlanta, GA 30324-0340, USA

ABSTRACT

(Hydro)thermal treatments of sewage sludge is a promising option that can simultaneously target safe waste disposal, energy recovery, and nutrient recovery/recycling. The speciation of phosphorus (P) in sludge is of great relevance to P reclamation/recycling and soil application of sludge-derived products, thus it is critical to understand the effects of different treatment techniques and conditions on P speciation. This study systematically characterized P speciation (i.e. complexation and mineral forms) in chars derived from pyrolysis and hydrothermal carbonization (HTC) of municipal sewage sludges. Combined sequential extraction and P K-edge X-ray absorption near edge structure (XANES) spectroscopy analysis revealed the dependence of P transformation on treatment conditions and metal composition in the feedstocks. Pyrolysis of sludges decreased the relative abundance of phytic acid while increased the abundance of Al-associated P. HTC thoroughly homogenized and exposed P for interaction with various metals/minerals, with the final P speciation closely related to the composition/speciation of metals and their affinities to P. Results from this study revealed the mechanisms of P transformation during (hydro)thermal treatments of sewage sludges, and might be applicable to other biosolids. It also provided fundamental knowledge basis for the design and selection of waste management strategies for better P (re)cycling and reclamation.

© 2016 Elsevier Ltd. All rights reserved.

1. Introduction

Global interests in sustainability are pressing for resource reclamation and recycling from waste streams, to which a significant fraction of critical elements consumed by human activities converges (Sartorius et al., 2012; Westerhoff et al., 2015). Current waste management systems are under the pressure to incorporate new technologies and strategies, and to integrate with energy and agricultural systems, to achieve societal sustainability (Brunner and Rechberger, 2015; Peccia and Westerhoff, 2015; Wang et al., 2015). One important research field is phosphorus (P) recycling/reclamation from various solid biowastes such as sewage sludge, due to the concern of phosphate resource depletion (Koppelaar and Weikard, 2013; Withers et al., 2015). The management of sewage sludge has long been a challenging task for both water treatment and solid waste management industries, due to the intrinsic high water content and large volume of sludges, as well as the presence of

various organic and inorganic contaminants (Escala et al., 2012; Rogers, 1996; Smith, 2009; Walter et al., 2006). In recent years, (hydro)thermal treatments (e.g., gasification, pyrolysis, hydrothermal liquefaction, and hydrothermal carbonization) have emerged as potential sustainable solutions to the sludge management problem, because these techniques can significantly decompose organic pollutants, reduce waste volume, and generate valuable by-products (e.g. pyrochar from thermal treatments or hydrochar from hydrothermal treatments) (Bridle and Pritchard, 2004; Escala et al., 2012; Kim and Parker, 2008; vom Eyser et al., 2014). The derived chars can be utilized as fuels for energy recovery, as soil amendments to improve soil quality, or as resources for P recycling and reclamation (He et al., 2013; Weber et al., 2014; Zhao et al., 2014). Numerous studies have investigated the energy recovery aspect (i.e. change of carbon speciation) from (hydro)thermal treatments of sludges (Kim et al., 2014; Parshetti et al., 2013; Zhao et al., 2014). Few studies have examined P behaviors during these treatments and the focus was mostly on the elemental migration between solid and liquid phases as well as total P recovery efficiency (Qian and Jiang, 2014; Zhai et al., 2014; Zhu et al., 2011).

The speciation (e.g. chemical state and physical distribution) of P intrinsically determines its solubility, mobility, and bioavailability. It is thus important to obtain detailed P speciation information during sludge treatment processes in order to understand the effects of different treatment techniques and conditions, as well as to select, design, and optimize sludge management strategies for specific P reclamation and recycling practices (e.g., extraction and reclamation of P from the products, direct application of the products as soil amendments). P can exist in different molecular moieties (e.g., orthophosphate, phosphonate, organic phosphates, and polyphosphate) and each moiety can present in different chemical states (e.g., be complexed with cations, adsorbed on other solid surfaces, incorporated into mineral phases, or precipitated as P-containing solids). Commonly available techniques for probing P speciation in complex and heterogeneous natural samples are ^{31}P nuclear magnetic resonance (NMR) spectroscopy, sequential extraction, and P K-edge X-ray absorption spectroscopy (XAS). However, each technique has its advantages and disadvantages and is not capable of fully characterizing P speciation in a complex and heterogeneous matrix (e.g. sewage sludge) alone (Cade-Menun, 2005; Doolette and Smernik, 2011; Ingall et al., 2011; Kizewski et al., 2011). It has been increasingly recognized that a holistic approach using these complementary techniques is necessary for obtaining detailed P speciation information (both molecular entity and their chemical states) and to explore P transformation pathways during sludge treatment.

In our recent work, we have characterized P molecular moieties in sewage sludges and their derived chars from (hydro)thermal treatments, and revealed the transformation pathways of different P moieties using ^{31}P solid state NMR as well as chemical extraction coupled with ^{31}P liquid NMR (Huang and Tang, 2015). In this study, we continue to characterize the chemical states of these different P moieties (e.g. complexation and mineralogy) during (hydro)thermal treatments of sewage sludge by coupling sequential extraction and P K-edge X-ray absorption near edge structure (XANES) analysis. Such strategy has been previously utilized to characterize P speciation in natural samples (Hashimoto and Watanabe, 2014; Kar et al., 2011; Kruse and Leinweber, 2008; Kruse et al., 2010), and has several advantages: 1) sequential extraction helps evaluate the mobility and availability of P in the solids; 2) at each extraction step, the P species being extracted into the solution phase and those remaining in the solid residues can be examined by XANES; 3) the correlation between operationally defined P fractions (by sequential extraction) and specific P species (by XANES) can be validated, which provides a better overview of P speciation.

Activated sludge and anaerobically digested sludge (hereafter referred to as anaerobic sludge) from the same wastewater treatment plant as in our previous study (Huang and Tang, 2015) were used as feedstocks for comparative evaluation of the influence of sludge source and metal contents on P speciation. Pyrolysis and hydrothermal carbonization (HTC) were selected as representative dry and wet thermochemical processes, respectively, to treat the sludges under different conditions (temperature and duration). This study, along with our previous study (Huang and Tang, 2015), is devoted to reveal the mechanistic transformation of P speciation during (hydro)thermal treatment of sludges, and ultimately provide fundamental knowledge basis for the design and selection of waste management strategies for better P reclamation and recycling.

2. Experimental approaches

2.1. Materials and treatments

Two types of sewage sludges (activated sludge and anaerobic sludge) were collected from F. Wayne Hill Water Resources Center (Gwinnett County, Atlanta, Georgia, USA). Details of sample collection, handling, and elemental composition were previously reported (Huang and Tang, 2015) and are also available in Supporting Information (SI) Text S1 and Table S1. The activated sludge represents sludge in its most unprocessed form, while the anaerobic sludge represents sludge that has experienced common processing (e.g. mixing of sludges from different units, dewatering, and anaerobic digestion) and has relatively higher metal contents than the activated sludge.

Pyrolysis and HTC were conducted on both the activated and anaerobic sludges. Details of the treatment conditions and sample labels are available in SI Text S1 and Table 1. Pyrolysis was conducted in a tube furnace (Thermo Scientific) under N_2 flow (~1 mL/s) at a range of temperatures (250—600 °C), with a heating and cooling rate of 200 °C/h and a soaking duration of 4 h. For each treatment condition, 1.0 g of freeze-dried sludge was added into a crucible and inserted into the glass tube of the furnace. All samples were processed in duplicates. The produced solid chars are hereafter referred to as pyrochar. For HTC treatment, wet sludge equivalent to ~1.8 g dry mass was weighted into a 20 mL Teflon lined stainless steel hydrothermal reactor (Parr instrument). Deionized water was then added to achieve a total weight of 12 g. The reactor was sealed and heated in an oven at 225 °C (which is at the middle of typical HTC conditions that range from 180 to 280 °C (Libra et al., 2011)) for 4 or 16 h, then allowed to naturally cool down to 50 °C in the oven. The produced solids (hereafter referred to as hydrochar) and the processed water were separated by centrifugation, and the hydrochar was immediately freeze-dried. The total mass recovery, processed water volume, and dried hydrochar mass were recorded. Pyrochars prepared at 250 and 450 °C (representing relatively low and high treatment temperatures, respectively) and hydrochars prepared at both 4 and 16 h were selected for subsequent characterizations (see below).

2.2. Sequential extraction

Sequential extractions of the raw sludges and their derived chars were conducted following the Hedley's method (Hedley et al., 1982). Specifically, 150 mg raw sludge or char was added to a 50 mL polypropylene centrifuge tube and sequentially extracted by 20 mL extraction solutions. The reaction tubes were constantly agitated by end-to-end shaking. The samples were first extracted with deionized water for 8 h, followed by 0.5 M $NaHCO_3$, 0.1 M NaOH, and 1.0 M HCl solutions, each lasting 16 h. Replicate set of experiments were conducted. At the end of each extraction step, one set of reaction was sacrificially taken down, and the solid and aqueous phases separated by filtration (0.45 μm). The solid residue was freeze-dried for XANES analysis, and the filtrate analyzed for P content.

2.3. P content quantification

P content in all liquid and solid samples was quantified using a combustion method. Specifically, freeze-dried solid samples were directly combusted at 600 °C for 2 h in a furnace, followed by an HCl extraction (1 M) for 16 h. To quantify P in the liquid extracts, due to the presence of organics, the solution was first dried in an oven at 50 °C, followed by the abovementioned combustion and acid extraction methods. Following the acid extraction, P content in the extract was analyzed as orthophosphate using the ascorbic acid assay (Murphy and Riley, 1962) on an UV—vis spectrophotometer (Carey 60, Agilent).

Table 1
Pyrolysis and HTC treatment conditions, sample label, and solid characteristics of the sludges (including solid recovery, solid P content, and P recovery). Solid recovery, solid P content, and P recovery data for pyrolysis treatments were from our previous work (Huang and Tang, 2015).

Sludge type	Treatment	Condition	Sample label	Solid recovery (%)	Solid P content (%)	P recovery (%)
Activated sludge	Raw	Freeze dried	Sludge	N/A	4.1 ± 0.1	N/A
	Pyrolysis	250 °C, 4 h	S250	69.1 ± 5.5	5.7 ± 0.1	95.8
	Pyrolysis	450 °C, 4 h	S450	45.6 ± 1.1	8.9 ± 0.1	98.2
	HTC	225 °C, 4 h	SHTC4h	55.2 ± 4.1	7.6 ± 0.1	101.3
	HTC	225 °C, 16 h	SHTC16h	48.5 ± 0.9	8.1 ± 0.1	89.3
Anaerobically digested sludge	Raw	Freeze dried	Ana	N/A	3.3 ± 0.1	N/A
	Pyrolysis	250 °C, 4 h	A250	72.2 ± 4.2	4.7 ± 0.1	103.1
	Pyrolysis	450 °C, 4 h	A450	47.2 ± 6.0	7.2 ± 0.2	103.2
	HTC	225 °C, 4 h	AHTC4h	55.6 ± 5.0	4.9 ± 0.1	81.7
	HTC	225 °C, 16 h	AHTC16h	49.8 ± 4.5	6.1 ± 0.1	95.5

2.4. P XANES analysis

P K-edge XANES data were collected at Beamline 14-3 at the Stanford Synchrotron Radiation Lightsource (SSRL), Menlo Park, CA. The raw sludges and their derived chars were ground into fine powders and brushed evenly onto P-free Kapton tapes. Excess powders were blown off to achieve a homogeneous and thin film. Sample-loaded tapes were then mounted to a sample holder. The sample chamber was maintained under He atmosphere at room temperature, and XANES data were collected in fluorescence mode using a PIPS detector. Energy calibration used $AlPO_4$ by setting the edge position (peak maxima of the first derivative) to be 2152.8 eV. Spectra for this reference sample were periodically collected to monitor possible energy shifting, which was not observed during the entire data collection period. XANES spectra were collected at 2100—2485 eV. Multiple scans were collected for each sample and averaged for further analysis.

Because Fe, Al, and Ca are the predominant metals present in these sludges, phosphate could either adsorb on their mineral phases or form solid precipitates (e.g. metal phosphate salts) with them. Therefore, the following groups of compounds were selected as reference compounds: (1) $FePO_4 \cdot 2H_2O$ (Sigma Aldrich) and phosphate sorbed on ferrihydrite, representing Fe-associated P; (2) $AlPO_4$ (VWR) and phosphate sorbed on γ-alumina (1 mM KH_2PO_4 with 100 mg γ-alumina in 20 mL suspension, pH 6.0, 3 h reaction, freeze dried), representing Al-associated P; (3) octacalcium phosphate (OctaCa) and hydroxylapatite (HydAP), representing Ca-associated P; (4) phytic acid (sodium salt, VWR), representing P associated with organic functional groups. These compounds have been shown to well represent P species in sludges and biosolids (Shober et al., 2006). Data collection for $FePO_4 \cdot 2H_2O$, $AlPO_4$, and phosphate sorbed alumina (P-alumina) used the same procedure as the sludge samples. Spectra of HydAp and phytic acid (PhyAc) were obtained from Werner and Prietzel (2015). Spectra of phosphate sorbed ferrihydrite (P-ferrihy) and OctaCa were kindly provided by Dr. Dean Hesterberg (North Carolina State University, USA). Since these spectra were obtained from different studies, their E_0 values were aligned with E_0 of the analogous samples from our current study. For example, Werner et al. also collected $AlPO_4$ spectra, and Dr. Hesterberg's reference data set also contained phytic acid (Na salt). XANES spectra of all reference compounds used in this study were present in Fig. S1.

Data analysis was performed using the softwares SIXPack and Ifeffit (Ravel and Newville, 2005; Webb, 2005). All spectra were carefully examined for energy calibration, merged, and normalized. Linear combination fitting (LCF) was conducted on the XANES spectra at energy range of −15 to +50 eV relative to the edge energy. E_0 values of reference compounds were allowed to float up to ±1 eV. All combinations of reference compounds were used to fit each sample. The goodness of fit was evaluated using the residual factor (R factor) and χ^2 values (Table S2), and the best fit was used.

3. Results and discussion

3.1. P speciation in raw sludges

Overall characteristics of the raw sludges and their derived chars, (hydro)thermal treatment parameters, and sample labels are presented in Table S1 and Table 1. In general, the physicochemical properties (e.g., elemental composition, physical states, and stability) of sewage sludges are dependent on many factors, such as sewage source, treatment techniques at wastewater treatment plants, as well as sludge collection and processing steps. Activated sludge directly from the biological treatment unit generally consists mostly of active granules (e.g. microbial cells and other organic/inorganic components) and P can present in different forms (in terms of both molecular entity and complexation form) and distribute heterogeneously, depending on the treatment techniques (Huang et al., 2015a, b; Majed et al., 2009; Zhang et al., 2013a, b). Anaerobic sludge receives both activated sludge and sludges from other units, and could have experienced extensive mechanical and thermal dewatering/drying and digestion processes.

LCF of P XANES spectra showed significant difference of P speciation between the activated and anaerobic sludges (Figs. 1 and 2, Table S3). If considering only species with >5% abundance, phytic acid (42%), $AlPO_4$ (34%), and alumina-adsorbed phosphate (15%) were the three main species identified in the activated sludge, while $AlPO_4$ (40%), phytic acid (20%), ferrihydrite-adsorbed phosphate (13%), octacalcium phosphate (OctaCa; 16%), and alumina-adsorbed phosphate (11%) were the main species identified in the anaerobic sludge. The P XANES results showed overall less organic P and more Fe/Ca-associated P species in the anaerobic sludge than activated sludge. This is most likely resulted from: 1) the release of intracellular or cell-bound P during the processing of activated sludge (e.g., organic matters typically experience extensive hydrolysis and homogenization processes during anaerobic digestion (Appels et al., 2008)), which might subsequently interact with metals such as Fe and Ca, 2) higher metal contents in anaerobic sludge than in activated sludge (Table S1). A previous study characterizing P speciation in sewage sludge using P K-edge XANES also showed that calcium phosphate, alumina/ferrihydrite adsorbed phosphate, and phytic acid were the main species, and their relative abundance depended on the sludge sources and the stabilization strategies the sludges had experienced (e.g., lime, Al salt, and Fe salt addition) (Shober et al., 2006).

3.2. P speciation changes during pyrolysis

After the pyrolysis of activated sludge, the most significant
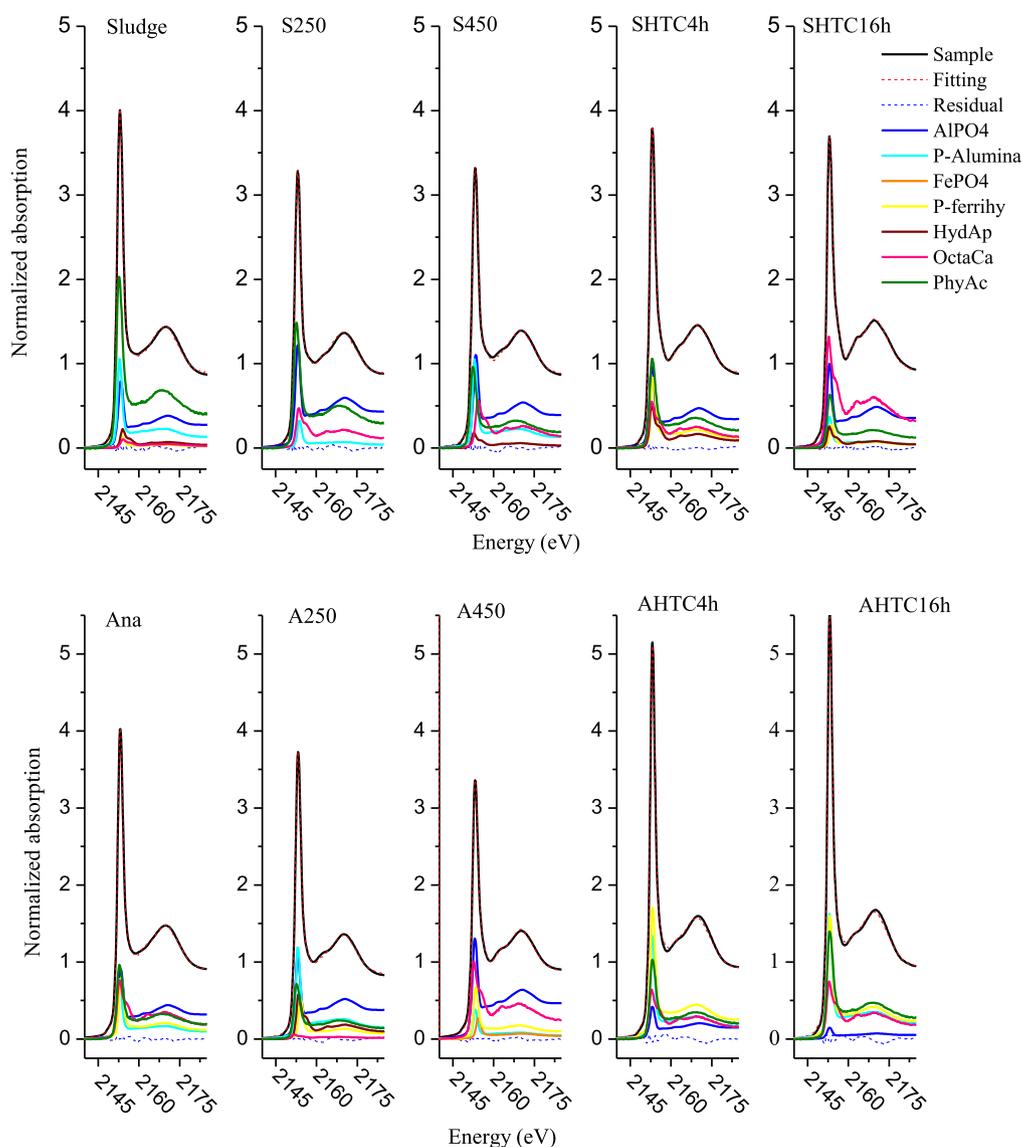
Fig. 1. Linear combination fittings of P XANES spectra of activated sludge, anaerobic sludge, and their pyrochars and hydrochars. Fitted components include AlPO₄, phosphate sorption on γ-alumina (P-Alumina), FePO₄, phosphate sorption on ferrihydrite (P-ferrihy), hydroxyapatite (HydAp), octacalcium phosphate (OctaCa), and phytic acid (PhyAc).

changes based on P XANES LCF results were the decrease of phytic acid (42%, 30%, and 20% for raw sludge, S250, and S450, respectively), as well as the increase of Al- and Ca-associated P (Figs. 1 and 2, Table S3). Al-associate P included contributions from both AlPO₄ and phosphate sorbed on alumina. Ca-associated P included contributions from both OctaCa and hydroxylapatite (HydAP). The relative abundance of OctaCa (and total Ca-associated P) increased from ∼2% (6.5%) for raw sludge to 9.6% (9.6%) and 12% (15.3%) for S250 and S450 pyrochars, respectively. The relative abundance of AlPO₄ (and total Al associated P) increased from 34% (49%) to 55% (59%) and 50% (65%) for sludge, S250, and S450, respectively.

After the pyrolysis of anaerobic sludge, the relative abundance of phytic acid also significantly decreased to 15% (sample A250) and 0% (sample A450), as compared to 20% in the raw anaerobic sludge (sample Ana). The relative abundance of Ca- and Al-associated P also increased after pyrolysis, although not monotonically. The relative abundance of OctaCa (and total Ca-associated P) was 16% (16%), 1.2% (12.4%), and 21% (21%) for Ana, A250, and A450, respectively. The relative abundance of AlPO₄ (and total Al-associated P) increased from 40% (52%) in the raw anaerobic

sludge (Ana) to 48% (65%) and 59% (65%) for A250 and A450, respectively. Pyrolysis seemed to have little effects on the relative abundance of Fe-associated P.

Overall, these results suggested that pyrolysis can significantly alter the complexation states of P, and the effects were dependent on pyrolysis temperature and feedstock characteristics (e.g. initial P speciation and metal composition). The decrease of phytic acid (or organics bound P) and increase of metal complexed P (mainly with Ca and Al) were most likely caused by two processes during pyrolysis: 1) the stripping of organic functional groups from the phosphate moiety and the subsequent substitution by metals, which appeared to be more significant at higher temperatures, and 2) in the case of activated sludge, the breakdown of polyphosphate into shorter chained polyphosphate, pyrophosphate, and orthophosphate that created additional P-O bonds available for metal complexation. Regarding the first process, it is well established that various reactions such as dehydration, deoxygenation, decarboxylation, aromatization, and polymerization are involved in the conversion of biomass to biochar (Demirbaş, 2000). The second process was substantiated by our previous study based on ³¹P NMR,
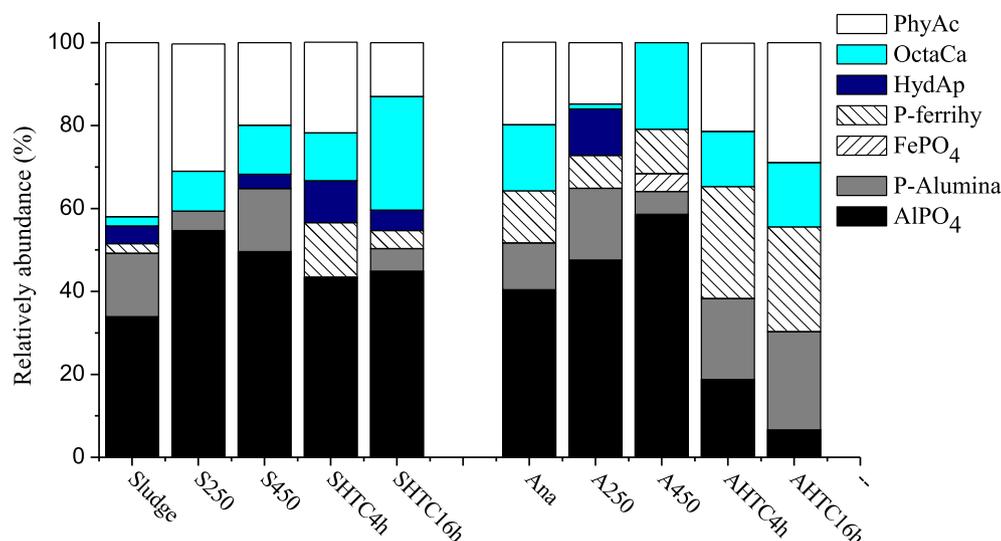
Fig. 2. Relative abundance of different P species in activated sludge (Sludge), anaerobically digested sludge (Ana), and their derived pyrochars and hydrochars, as quantified by linear combination fitting of their P XANES spectra. Reference library used for fitting include phytic acid (PhyAc), octacalcium phosphate (OctaCa), hydroxyapatite (HydAp), phosphate sorption on ferrihydrite (P-ferrihy), $FePO_4$, phosphate sorption on γ-alumina (P-Alumina), and $AlPO_4$.

which demonstrated the breakdown of polyphosphate into pyro-phosphate and shorter chained polyphosphates after pyrolysis of activated sludge (Table 2) (Huang and Tang, 2015). Similar decrease in organic P after pyrolysis was also observed for manures based on chemical extraction (Dai et al., 2015).

3.3. P speciation changes during hydrothermal carbonization

Our previous work demonstrated that the main P moeity in hydrochars from HTC treatment was orthophosphate (Table 2), regardless of the feedstock (activated sludge vs. anaerobic sludge) (Huang and Tang, 2015). Therefore, for HTC treatment, we only need to focus on examining the complexation states of ortho-phosphate after HTC treatment.

Based on P XANES LCF results, HTC significantly altered the P speciation in both activated and anaerobic sludges, with similarities and differences as discussed below (Figs. 1 and 2, Table S3). For activated sludge, the relative abundance of Fe-associated P (all as ferrihydrite adsorbed phosphate) increased after HTC, from 2.3% in raw activated sludge to 13% and 4.4% in its HTC4h and HTC16h hydrochars, respectively. Similar to the effects of pyrolysis, the relative abundance of phytic acid decreased, from 42% in raw sludge to 22% and 13% in SHTC4h and SHTC16h, respectively. The relative abundance of Ca-associated P also increased, with the abundance of

OctaCa (and total Ca-associated P) increasing from 2.2% (6.6%) for raw sludge to 11.5% (21.6%) and 27% (32%) for SHTC4h and SHTC16h, respectively. In contrast to the increase of total Al-associated P (and $AlPO_4$) after pyrolysis, the abundance of total Al-associated P remained unchanged after HTC (49%, 43%, and 50% for raw sludge, SHTC4h, and SHTC16h, respectively), although there were slight increases in $AlPO_4$ (34%, 43%, and 45% for raw sludge, SHTC4h, and SHTC16h, respectively).

For anaerobic sludge, all the Fe-associated P existed as ferrihy-drite adsorbed phosphate, and its relative abundance increased after HTC from 13% for raw anaerobic sludge (sample Ana) to 27% and 25% for AHTC4h and AHTC16h, respectively. The abundance of total Al-associated P (and $AlPO_4$) decreased from 52% (40%) for Ana to 38% (19%) and 30% (7%) for AHTC4h and AHTC16h, respectively, while that of alumina adsorbed P increased from 11% for Ana to 20% and 24%, for AHTC4h and AHTC16h, respectively. Contrary to that of activated sludge and the effects of pyrolysis, there was a slight increase in the relative abundance of phytic acid in the hydrochars of anaerobic sludge (21% and 29% for AHTC4h and AHTC16h, respectively, compared to 20% for Ana). The relative abundance of OctaCa remained unchanged (13% and 16% for AHTC4h and AHTC16h, respectively, compared to 16% for Ana).

The P speciation changes during HTC may be collectively controlled by the composition and states of metals with high

Table 2
Summary of findings from chemical extraction, ^{31}P NMR (Huang and Tang, 2015), and P K-edge XANES analysis of the raw and (hydro)thermal treated sludges.

Technique	Feedstock	Treatment		
		Raw (untreated)	Pyrolysis	HTC
Chemical extraction	Sludge	43% by H_2O and $NaHCO_3$, ~30% by NaOH, 8% by HCl	P stabilized. 40% by NaOH, 49% by HCl	P stabilized. ~70–80% by NaOH, the rest by HCl
	Ana	14% by H_2O and $NaHCO_3$, ~60% by NaOH, ~20% by HCl	P stabilized. 49% by NaOH, 46% by HCl	P stabilized. ~40–65% by NaOH, the rest by HCl
^{31}P NMR	Sludge	Dominated by orthoP and polyP. $P_{obs} > 90\%$	Dominated by orthoP, pyroP and polyP. $P_{obs} > 85\%$ (250 & 450 °C)	OrthoP. $P_{obs} \sim 31\%$
	Ana	Dominated by orthoP. P_{obs} 40%	Dominated by orthoP	Dominated by orthoP
P K-edge XANES	Sludge	Phytic acid (42%), Al-P (49%)	Phytic acid ↓, Al-P ↑, Ca-P ↑	Phytic acid ↓, Fe-P ↑, Ca-P ↑
	Ana	Phytic acid (20%), Al-P (51%), Fe-P (13%), Ca-P (16%)	Phytic acid ↓, Al-P ↑	Fe-P ↑, Al-P ↓

Note: Sludge (activated sludge), Ana (anaerobically digested sludge), orthoP (orthophosphate), polyP (polyphosphate), pyroP (pyrophosphate), P_{obs} (NMR observable phosphorus), Al-P (Al-associated P), Fe-P (Fe-associated P), Ca-P (Ca-associated P).

affinity to phosphate and the thermochemical reactions occurred during HTC. First of all, reactions occurred during HTC may homogenize phosphates and expose them to various metals and minerals, especially for activated sludge. During HTC, reactions such as hydrolysis, decarboxylation, and polymerization were found to be involved in the transformation of biomass (Funke and Ziegler, 2010). These reactions were responsible for the hydrolysis of polyphosphate into orthophosphate for activated sludge and exposed the intracellular and organic-bound P to metals such as Ca and Fe, to certain extent similar to the effects of anaerobic digestion. This explains the decrease of phytic acid and increasing abundance of Ca- and Fe-associated P after HTC of activated sludge, as well as the similarity in P speciation between hydrochars of activated sludge and anaerobic sludge (Fig. 2). For HTC of anaerobic sludge, since P in the raw sludge has been relatively homogenized, the magnitude of alterations (changes in only the relative abundance of Fe- and Al-associated P) was much smaller than that for activated sludge. Secondly, metals such as Fe, Ca, and Al have higher affinity to phosphate than metals such as Na, K, and Mg, and are more abundant than metals such as Cu and Zn, thus phosphate are more likely associated with them. Moreover, the relative abundance and forms of these metals determine the P association stoichiometry and capacity (e.g., Fe mostly present as hydroxide minerals and bound P as surface adsorbed form, while Ca formed Ca-phosphate minerals in competition with its carbonate and sulfate mineral phases). Since there was a much higher Fe content in anaerobic sludge (~9%) than in activated sludge (~3.6%), higher Fe association with P was found in anaerobic sludge and its hydrochars, compared to that of activated sludge and its chars.

3.4. Chemical fractionation by sequential extraction

Hedley's sequential extraction method involves four wet extraction steps, each indicative of the relative mobility and/or chemical states of P: DI water (readily soluble P, most labile), $NaHCO_3$ (soluble and desorbed P, moderately labile), NaOH (Fe/Al-associated P that is soluble or can be desorbed under alkaline conditions), and HCl (insoluble phosphate salts and minerals). Although this method has been extensively applied for the indirect determination of P speciation, few studies had evaluated whether the chemically fractionated P pools were equivalent to certain P chemical species (Hashimoto and Watanabe, 2014; Kar et al., 2011; Kruse and Leinweber, 2008; Kruse et al., 2010; Takamoto and Hashimoto, 2014). Here, we quantified the P partition in different extraction solutions and characterized the P speciation in the solid residues after each sequential extraction step, in an attempt to explore the relationships between P speciation estimated by P K-edge XANES and the mobility/fractionation information probed by sequential extraction.

Sequential extraction showed different P fractionation behaviors between the two sludges and after their pyrolysis and HTC treatments (Fig. 3 and Table S4). For activated sludge, a significant amount of P partitioned in the H_2O (26%) and $NaHCO_3$ (17%) fractions, and these two fractions became negligible after pyrolysis and HTC processing (<2%). After pyrolysis at 450 °C, the NaOH and HCl fractions increased respectively to 40% and 49%, compared to 31% and 7% for raw sludge, respectively. Although HTC increased P partitioning in both NaOH and HCl fractions, the enhancement was more significant for the NaOH fraction (~71% and 81% for SHTC4h and SHTC16h, respectively) than for the HCl fraction (~28% and 24% for SHTC4h and SHTC16h, respectively).

For anaerobic sludge, the relatively mobile H_2O (6%) and $NaHCO_3$ (8%) fractions were much smaller compared to those of activated sludge, and both decreased significantly after pyrolysis and HTC treatment. After pyrolysis at 450 °C, the NaOH fraction
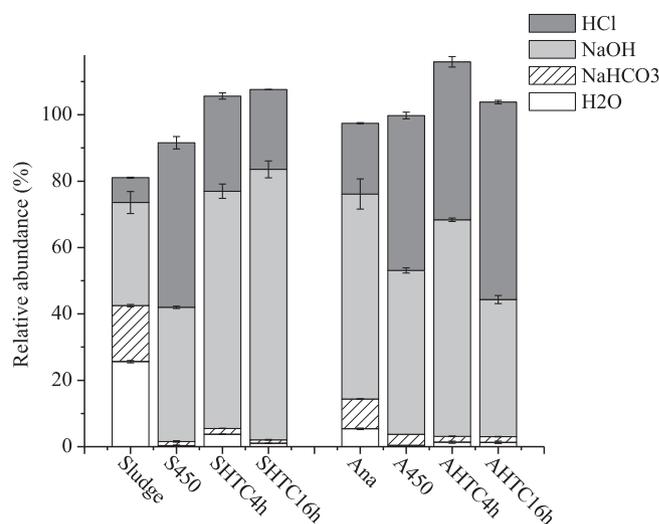
Fig. 3. Distribution of P in sequential extracts of sludges and their derived pyrochars and hydrochars. The relative percentage of each component was calculated by normalizing the P amount in each extract (20 mL) by the total P in the solids (150 mg) used in the extraction. Each data was the average of results from two independent extraction experiments. Total sums did not equal to 100%, due to the remaining P in the residue and analytical errors.

decreased from 62% to 49% and the HCl fraction increased from 21% to 47%. The significant enhancement in the HCl fraction after pyrolysis was also similar to the pyrolysis of activated sludge. HTC did not significantly increase the NaOH fraction in the hydrochars of anaerobic sludge (65% and 41% for AHTC4h and AHTC16h, respectively, compared to 62% for the raw anaerobic sludge), but enhance the HCl fraction (47% and 57% for AHTC4h and AHTC16h, respectively, compared to 21% for the raw anaerobic sludge).

These results suggested that both pyrolysis and HTC substantially stabilized P during the treatment processes, with the stabilization mechanism being different and feedstock-dependent. P stabilization by pyrolysis have been observed in a previous study on the pyrolysis of sewage sludge (Qian and Jiang, 2014). P immobilized after HTC treatment was also observed for cow manure, where the water-extractable P (WEP) and mehlich-3-extractable P (MEP) decreased from ~50% and 65% in the raw feedstock to ~8% and 20% after HTC treatment, respectively (Dai et al., 2015). To further elucidate the stabilization mechanism and the chemical nature of acid/base partitioning of different P species, we conducted P XANES and LCF analysis on the solid residues after each extraction step (Fig. 4). The obtained P speciation information was also compared to the speciation fractions assuming no loss during extraction to evaluate the relative extraction extent of each P species (Table S5).

During H_2O extraction, $AlPO_4$ was the main P species being preferentially extracted for activated sludge, if neglecting the small contribution from ferrihydrite adsorbed P and HydAP (2.3% and 4.3%, respectively). $AlPO_4$, alumina adsorbed phosphate, and OctaCa were all preferentially extracted for anaerobic sludge.

During $NaHCO_3$ extraction, $AlPO_4$, OctaCa, and phytic acid were the main P species preferentially extracted from activated sludge. OctaCa and phytic acid were the main species extracted from anaerobic sludge. Since H_2O and $NaHCO_3$ did not extract significant amounts of P from the pyrochars and hydrochars, data of the solid residues were not presented. $AlPO_4$, alumina adsorbed P, ferrihydrite adsorbed P, and phytic acid were extracted during NaOH extraction of the two raw sludges.

For the char samples (i.e. pyrochars from pyrolysis and hydrochars from HTC), the changes following H_2O-$NaHCO_3$-NaOH extraction were not always consistent for all the samples. For all the
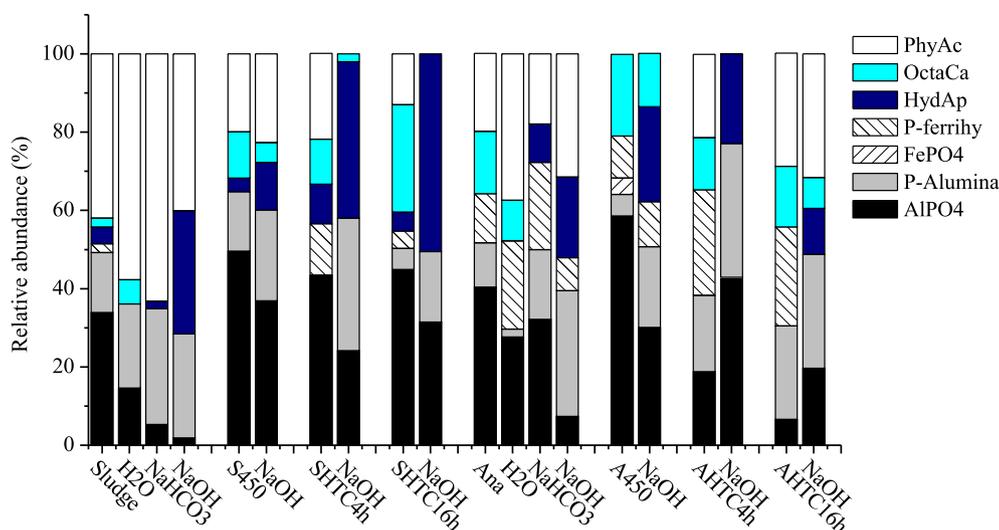
Fig. 4. Relative abundance of different P species in sludges and their chars, as well as the solid residuals after each sequential extraction step of the sludges and chars, as quantified by linear combination fitting of their P XANES spectra. Due to low P content in the final HCl extracted residue and the resulting poor XANES signal, LCF was not performed on HCl extracted residues.

char samples produced by pyrolysis and HTC, the relative abundance of ferrihydrite adsorbed PO_4 significantly decreased or completely disappeared after NaOH extraction, especially for the hydrochar samples (Fig. 4). $AlPO_4$ (except for AHTC16h), OctaCa, and phytic acid were all extracted during NaOH extraction for all the char samples, with varied degrees of extraction. Although the alumina adsorbed P species in the hydrochar of anaerobic sludge was extracted by NaOH, that in all pyrochars and hydrochars of activated sludge was not extracted (or even enhanced). Compared to the raw sludges, whose $AlPO_4$, alumina adsorbed phosphate, OctaCa, and phytic acid could be extracted to different degrees by H_2O or $NaHCO_3$, these species in the chars were relatively more stable and can only be extracted by NaOH or HCl, suggesting that physical constraints (e.g. embedment of P species into the char structure) may also play a role in P stabilization.

In general, ferrihydrite-adsorbed P and Al-associated P was preferentially extracted during the NaOH step, which was chemically sound and consistent with previous results for soil samples (Kar et al., 2011). Phytic acid was also mostly extracted only during the NaOH step. Ca-associated P remained relatively immobile throughout the H_2O-$NaHCO_3$-NaOH steps, which was also chemically sound and consistent with the general low solubility of Ca-P minerals (e.g. apatite) in these solutions. One interesting observation was that, although HydAP was not identified (or only constituted a very small fraction) in the raw sludge and char samples, it was present abundantly and disproportionally in the residues after NaOH extraction. Amorphous and more crystalline Ca phosphates differ in the relative intensity of the post-edge shoulder and second peak (Fig. S1) (Oxmann, 2014), thus it was possible that OctaCa (and less crystalline Ca phosphate) transformed into HydAP during the sequential extraction process. This was also in agreement with the fact that HydAP is more stable than OctaCa, and only dissolves in HCl, instead of NaOH.

3.5. Combined analysis of NMR, XANES, and chemical extraction results

As previously discussed, the main techniques available for speciating P in environmental solid matrices (i.e. liquid and solid state ^{31}P NMR, P K-edge XANES, and chemical extraction) each has intrinsic limits and strengths. Therefore, below we comparatively analyzed results using these techniques from this work and our previous study (Huang and Tang, 2015), in order to obtain a more comprehensive understanding of P speciation transformation during sludge treatment, to validate the findings, and to identify any discrepancies and their causes (Table 2).

First, the increasing metal association (especially Ca and Fe) with P after anaerobic digestion and HTC treatment from P XANES is consistent with solid state NMR results showing decreasing P observation. Less P was observable by NMR in anaerobic sludge (~40%) and the hydrochar of active sludge (31%) than in the raw activated sludge (>90%) (Table 2) (Huang and Tang, 2015). More P were associated with Fe in hydrochars derived from anaerobic sludge (>25%) than that from activated sludge (13% in SHTC4h) due to higher Fe content in anaerobic sludge than in activated sludge. In hydrochars from activated sludge, P associations with Al and Ca were more than those in hydrochars from anaerobic sludge.

Second, liquid NMR was able to identify and quantify different P entities in the extracts from activated sludge and its pyrochars (pyrophosphate and polyphosphate accounted for ~30–40%) (Huang and Tang, 2015). However it was challenging for P XANES to distinguish and identify the complexation states for these entities, as their local coordination environments has similar PO_4 tetrahedra (structure of representative organic and inorganic P species for our system are illustrated in Fig. S2 and XANES spectra for representative organic P are present in Figs. S1 and S3). Therefore, it was difficult to deconvolute the chemical states of orthophosphate and polyphosphate in the activated sludge and its pyrochars using P XANES. Compared to Ca- and Fe-associated P whose P XANES spectra have distinctive pre-edge and post-edge features, the P XANES spectra of $AlPO_4$, alumina adsorbed phosphate or polyphosphate, and phytic acid are relatively featureless and differ in the white line intensity (Fig. S1). It is possible that the P XANES LCF fitted phytic acid, aluminum phosphate, and alumina adsorbed phosphate species might have partial contributions from polyphosphate moiety (e.g. presence of aluminum polyphosphate or alumina adsorbed polyphosphate species).

Third, in addition to the evaluation of P mobility, sequential extraction also helped validate LCF fitting results and identify possible uncertainties. P stabilization and different partition behaviors revealed by sequential extraction were qualitatively consistent with P species transformation revealed by P XANES. For

example, P stabilization (the more significant increase of the HCl fraction than that of the NaOH fraction) after pyrolysis were qualitatively in agreement with XANES results, which showed increased abundance of OctaCa and AlPO$_4$ after pyrolysis (these salts generally dissolve in HCl instead of NaOH). The presence and increasing abundance of ferrihydrite adsorbed P after HTC treatment was consistent with the disappearance of ferrihydrite adsorbed P during NaOH extraction. In addition to the abovementioned results, the general persistence of Ca-associated P after H$_2$O-NaHCO$_3$-NaOH steps was also consistent with the LCF of XANES data. However, sequential extraction also suggested that the identification and quantification of certain species by P XANES should be evaluated with caution. Using AlPO$_4$ and phytic acid as examples, although AlPO$_4$ is not soluble in water and NaHCO$_3$, it was shown to be extractable during sequential extraction of the raw sludges. Phytic acid was not identified in the extracts of these samples using liquid ^{31}P NMR, yet accounted for a significant portion of total P by LCF of XANES data. These discrepancies were possibly due to (1) the limited reference compound library (for complex and heterogeneous environmental samples such as sewage sludge, it is almost impossible to establish a reference compound library that covers all the P species), (2) the intrinsic insensitivity of P XANES in distinguishing structurally similar species (as discussed previously, species with less distinctive features in their XANES spectra could result in large fitting uncertainties), and (3) the errors associated with LCF as a mathematical method (typically error of LCF is ~10% even for systems with predetermined mix of pure compounds (Werner and Prietzel, 2015)).

The combined sequential extraction and XANES analysis also helped evaluating the matrix effect on P mobility, which is manifested in the different extraction efficiencies for certain P species between different samples. For example, ferrihydrite adsorbed P was completely extracted by NaOH for most samples, but not for anaerobic sludge and its pyrochars (similarly the sample-dependent NaOH extraction efficiency for phytic acid and alumina-adsorbed P).

In summary, compared to most previous studies on environmental samples (e.g., soil, sediment, and biosolids) using P K-edge XANES and LCF without cross-validation, our combined NMR, sequential extraction, and P XANES analysis provided an in-depth evaluation of P speciation in complex matrices and also identified uncertainties associated with each technical approach.

4. Conclusions

Although biomass and organic waste treatments with pyrolysis and hydrothermal techniques have been extensively studied, the focus was mainly on the transformation of carbon. The transformation of other elements such as P, N, and metals were much less studied. Combined results from this study and our previous work provided a mechanistic understanding of the transformation of P speciation (both molecular entities and complexation states) during (hydro)thermal treatment of sewage sludge:

- Coupled sequential extraction and P XANES analysis indicated the immobilization of P after (hydro)thermal treatments, due to the forming of relatively stable Ca- and Fe-associated P species as well as potential physical constraints.
- Speciation changes following treatments and the relative abundance of the species were dependent on both treatment techniques and feedstock composition.
- Coupling sequential extraction and P XANES measurements enabled the validation of speciation results and identification of potential analytical and statistical uncertainties associated with each technique alone.

Since the speciation (both chemical and physical) of P largely determines its mobility and availability, understanding the effects of treatment techniques and conditions on P speciation in the treatment products has great implications for tuning the treatment techniques and conditions for better P reclamation and recycling. The results and methodology can also be generalized and applied to (hydro)thermal treatments of other organic wastes and the investigation of other elements.

Appendix A. Supplementary data

Supplementary data related to this article can be found at http://dx.doi.org/10.1016/j.watres.2016.05.029.

References

Appels, L., Baeyens, J., Degrève, J., Dewil, R., 2008. Principles and potential of the anaerobic digestion of waste-activated sludge. Prog. Energy Combust. Sci. 34 (6), 755–781.

Bridle, T., Pritchard, D., 2004. Energy and nutrient recovery from sewage sludge via pyrolysis. Water Sci. Technol. 50 (9), 169–175.

Brunner, P.H., Rechberger, H., 2015. Waste to energy — key element for sustainable waste management. Waste Manag. 37, 3–12.

Cade-Menun, B.J., 2005. Characterizing phosphorus in environmental and agricultural samples by 31P nuclear magnetic resonance spectroscopy. Talanta 66 (2), 359–371.

Dai, L.C., Tan, F.R., Wu, B., He, M.X., Wang, W.G., Tang, X.Y., Hu, Q.C., Zhang, M., 2015. Immobilization of phosphorus in cow manure during hydrothermal carbonization. J. Environ. Manag. 157, 49–53.

Demirbaş, A., 2000. Mechanisms of liquefaction and pyrolysis reactions of biomass. Energy Convers. Manag. 41 (6), 633–646.

Doolette, A.L., Smernik, R.J., 2011. In: Bunemann, E.K., Oberson, A., Frossard, E. (Eds.), Phosphorus in Action: Biological Processes in Soil Phosphorus Cycling, pp. 3–36.

Escala, M., Zumbühl, T., Koller, C., Junge, R., Krebs, R., 2012. Hydrothermal carbonization as an energy-efficient alternative to established drying technologies for sewage sludge: a feasibility study on a laboratory scale. Energy Fuels 27 (1), 454–460.

Funke, A., Ziegler, F., 2010. Hydrothermal carbonization of biomass: a summary and discussion of chemical mechanisms for process engineering. Biofuels Bioprod. Biorefining 4 (2), 160–177.

Hashimoto, Y., Watanabe, Y., 2014. Combined applications of chemical fractionation, solution P-31-NMR and P K-edge XANES to determine phosphorus speciation in soils formed on serpentine landscapes. Geoderma 230, 143–150.

He, C., Giannis, A., Wang, J.Y., 2013. Conversion of sewage sludge to clean solid fuel using hydrothermal carbonization: hydrochar fuel characteristics and combustion behavior. Appl. Energy 111, 257–266.

Hedley, M.J., Stewart, J., Chauhan, B., 1982. Changes in inorganic and organic soil phosphorus fractions induced by cultivation practices and by laboratory incubations. Soil Sci. Soc. Am. J. 46 (5), 970–976.

Huang, R., Tang, Y., 2015. Speciation dynamics of phosphorus during (Hydro)Thermal treatments of sewage sludge. Environ. Sci. Technol. 49 (24), 14466–14474.

Huang, W.L., Cai, W., Huang, H., Lei, Z.F., Zhang, Z.Y., Tay, J.H., Lee, D.J., 2015a. Identification of inorganic and organic species of phosphorus and its bioavailability in nitrifying aerobic granular sludge. Water Res. 68, 423–431.

Huang, W.L., Huang, W.W., Li, H.F., Lei, Z.F., Zhang, Z.Y., Tay, J.H., Lee, D.J., 2015b. Species and distribution of inorganic and organic phosphorus in enhanced phosphorus removal aerobic granular sludge. Bioresour. Technol. 193, 549—552.

Ingall, E.D., Brandes, J.A., Diaz, J.M., de Jonge, M.D., Paterson, D., McNulty, I., Elliott, W.C., Northrup, P., 2011. Phosphorus K-edge XANES spectroscopy of mineral standards. J. Synchrotron Radiat. 18, 189—197.

Kar, G., Hundal, L.S., Schoenau, J.J., Peak, D., 2011. Direct chemical Speciation of P in sequential chemical extraction residues using P K-Edge X-ray absorption near-edge structure spectroscopy. Soil Sci. 176 (11), 589—595.

Kim, D., Lee, K., Park, K.Y., 2014. Hydrothermal carbonization of anaerobically digested sludge for solid fuel production and energy recovery. Fuel 130 (0), 120—125.

Kim, Y., Parker, W., 2008. A technical and economic evaluation of the pyrolysis of sewage sludge for the production of bio-oil. Bioresour. Technol. 99 (5), 1409—1416.

Kizewski, F., Liu, Y.T., Morris, A., Hesterberg, D., 2011. Spectroscopic approaches for phosphorus speciation in soils and other environmental systems. J. Environ. Qual. 40 (3), 751—766.

Koppelaar, R.H.E.M., Weikard, H.P., 2013. Assessing phosphate rock depletion and phosphorus recycling options. Glob. Environ. Change 23 (6), 1454—1466.

Kruse, J., Leinweber, P., 2008. Phosphorus in sequentially extracted fen peat soils: a K-edge X-ray absorption near-edge structure (XANES) spectroscopy study. J. Plant Nutr. Soil Sci. 171 (4), 613—620.

Kruse, J., Negassa, W., Appathurai, N., Zuin, L., Leinweber, P., 2010. Phosphorus speciation in sequentially extracted agro-industrial by-products: evidence from X-ray absorption near edge structure spectroscopy. J. Environ. Qual. 39 (6), 2179—2184.

Libra, J.A., Ro, K.S., Kammann, C., Funke, A., Berge, N.D., Neubauer, Y., Titirici, M.-M., Führner, C., Bens, O., Kern, J., Emmerich, K.H., 2011. Hydrothermal carbonization of biomass residuals: a comparative review of the chemistry, processes and applications of wet and dry pyrolysis. Biofuels 2 (1), 71—106.

Majed, N., Matthäus, C., Diem, M., Gu, A.Z., 2009. Evaluation of intracellular poly-phosphate dynamics in enhanced biological phosphorus removal process using Raman microscopy. Environ. Sci. Technol. 43 (14), 5436—5442.

Murphy, J., Riley, J.P., 1962. A modified single solution method for the determination of phosphate in natural waters. Anal. Chim. Acta 27 (0), 31—36.

Oxmann, J.F., 2014. Technical note: an X-ray absorption method for the identifica-tion of calcium phosphate species using peak-height ratios. Biogeosciences 11 (8), 2169—2183.

Parshetti, G.K., Liu, Z.G., Jain, A., Srinivasan, M.P., Balasubramanian, R., 2013. Hy-drothermal carbonization of sewage sludge for energy production with coal. Fuel 111, 201—210.

Peccia, J., Westerhoff, P., 2015. We should expect more out of our sewage sludge. Environ. Sci. Technol. 49 (14), 8271—8276.

Qian, T.-T., Jiang, H., 2014. Migration of phosphorus in sewage sludge during different thermal treatment processes. ACS Sustain. Chem. Eng. 2 (6), 1411—1419.

Ravel, Á., Newville, M., 2005. ATHENA, ARTEMIS, HEPHAESTUS: data analysis for X-ray absorption spectroscopy using IFEFFIT. J. Synchrotron Radiat. 12 (4), 537—541.

Rogers, H.R., 1996. Sources, behaviour and fate of organic contaminants during sewage treatment and in sewage sludges. Sci. Total Environ. 185 (1—3), 3—26.

Sartorius, C., von Horn, J., Tettenborn, F., 2012. Phosphorus recovery from wastewater—expert survey on present use and future potential. Water Environ. Res. 84 (4), 313—322.

Shober, A.L., Hesterberg, D.L., Sims, J.T., Gardner, S., 2006. Characterization of phosphorus species in biosolids and manures using XANES spectroscopy. J. Environ. Qual. 35 (6), 1983—1993.

Smith, S.R., 2009. A critical review of the bioavailability and impacts of heavy metals in municipal solid waste composts compared to sewage sludge. Environ. Int. 35 (1), 142—156.

Takamoto, A., Hashimoto, Y., 2014. Assessment of Hedley's sequential extraction method for phosphorus forms in biosolids using P K-edge x-ray absorption near-edge structure spectroscopy. Chem. Lett. 43 (11), 1696—1697.

vom Eyser, C., Palmu, K., Otterpohl, R., Schmidt, T.C., Tuerk, J., 2014. Determination of pharmaceuticals in sewage sludge and biochar from hydrothermal carbon-ization using different quantification approaches and matrix effect studies. Anal. Bioanal. Chem. 1—10.

Walter, I., Martínez, F., Cala, V., 2006. Heavy metal speciation and phytotoxic effects of three representative sewage sludges for agricultural uses. Environ. Pollut. 139 (3), 507—514.

Wang, X., McCarty, P.L., Liu, J., Ren, N.Q., Lee, D.J., Yu, H.Q., Qian, Y., Qu, J., 2015. Probabilistic evaluation of integrating resource recovery into wastewater treatment to improve environmental sustainability. Proc. Natl. Acad. Sci. U.S.A. 112 (5), 1630—1635.

Webb, S., 2005. SIXpack: a graphical user interface for XAS analysis using IFEFFIT. Phys. Scr. 2005 (T115), 1011.

Weber, B., Stadlbauer, E.A., Schlich, E., Eichenauer, S., Kern, J., Steffens, D., 2014. Phosphorus bioavailability of biochars produced by thermo-chemical conver-sion. J. Plant Nutr. Soil Sci. 177 (1), 84—90.

Werner, F., Prietzel, J., 2015. Standard protocol and quality assessment of soil phosphorus speciation by P K-edge XANES spectroscopy. Environ. Sci. Technol. 49 (17), 10521—10528.

Westerhoff, P., Lee, S., Yang, Y., Gordon, G.W., Hristovski, K., Halden, R.U., Herckes, P., 2015. Characterization, recovery opportunities, and valuation of metals in municipal sludges from U.S. wastewater treatment plants nationwide. Environ. Sci. Technol. 49 (16), 9479—9488.

Withers, P.J.A., Elser, J.J., Hilton, J., Ohtake, H., Schipper, W.J., van Dijkf, K.C., 2015. Greening the global phosphorus cycle: how green chemistry can help achieve planetary P sustainability. Green Chem. 17 (4), 2087—2099.

Zhai, Y., Xiang, B., Chen, H., Xu, B., Zhu, L., Li, C., Zeng, G., 2014. Recovery of phos-phorus from sewage sludge in combination with the supercritical water pro-cess. Water Sci. Technol. 70 (6), 1108—1114.

Zhang, H.L., Fang, W., Wang, Y.-P., Sheng, G.P., Xia, C.W., Zeng, R.J., Yu, H.Q., 2013a. Species of phosphorus in the extracellular polymeric substances of EBPR sludge. Bioresour. Technol. 142 (0), 714—718.

Zhang, H.L., Fang, W., Wan, Y.P., Sheng, G.P., Zeng, R.J., Li, W.W., Yu, H.Q., 2013b. Phosphorus removal in an enhanced biological phosphorus removal process: roles of extracellular polymeric substances. Environ. Sci. Technol. 47 (20), 11482—11489.

Zhao, P.T., Shen, Y.F., Ge, S.F., Yoshikawa, K., 2014. Energy recycling from sewage sludge by producing solid biofuel with hydrothermal carbonization. Energy Convers. Manag. 78, 815—821.

Zhu, W., Xu, Z.R., Li, L., He, C., 2011. The behavior of phosphorus in sub- and super-critical water gasification of sewage sludge. Chem. Eng. J. 171 (1), 190—196.